# Recovery of the training effect in exchange bias systems within a coherent rotation model

B. F. Miao, J. H. Ai, L. Sun, B. You, An Hu, and H. F. Ding*

*National Laboratory of Solid State Microstructures and Department of Physics, Nanjing University, 22 Hankou Rd., Nanjing 210093, China*

(Received 20 July 2010; revised manuscript received 21 September 2010; published 27 October 2010)

Brems *et al.*, [Phys. Rev. Lett. **95**, 157202 (2005)] reported that the training effect in Co/CoO bilayers can be recovered by performing a hysteresis loop with an in-plane field perpendicular to the initial cooling field without raising the temperature above the Néel temperature. We performed numerical simulations of this effect within the coherent rotation model with multiple antiferromagnetic (AFM) easy axes. Both the ferromagnetic (FM) and AFM layers are divided into multi domains, and each FM domain couples with one AFM domain. In combination with the anisotropic magnetoresistance calculation, we find a strong dependence of the training recovery effect on the magnitude of the perpendicular field, in good agreement with the experimental findings.

DOI: 10.1103/PhysRevB.82.134442 PACS number(s): 75.30.Gw, 75.60.−d, 73.43.Qt

## I. INTRODUCTION

When a ferromagnetic- (FM-) antiferromagnetic (AFM) bilayer is cooled in a magnetic field through the Néel temperature ($T_N$) of the AFM layer, an unidirectional magnetic anisotropy can be induced, which is referred to the exchange bias. This effect was discovered about half a century ago by Meiklejohn and Bean.[1] The exchange coupling between the AFM and FM layers gives rise to a shift and/or a broadening of the FM hysteresis loop along the magnetic field axis. Through the exchange coupling, the AFM layers can pin the FM layers and thus establish a reference magnetization direction in spintronic devices, such as magnetic field sensors and read heads used for high density magnetic recording.[2,3] Though it has been widely used in many applications, some of the basic mechanisms of the exchange bias remain to be unveiled.[3–5]

Shortly after the discovery of the exchange bias, it was found in some exchange bias systems that the coercivity in the hysteresis loop can decrease with repeated cycling of the magnetic field.[6] This effect is called the training effect. Experimentally, it has been found that there are two distinct types of training effect, one between the first and second loop and the other one involving a continuously decreasing coercivity with increasing number of loops. Interestingly, for an epitaxial system, these two types effects can be well described by a phenomenological theory.[7,8] It is generally believed that the origin of the training effect is related to the change in the spin state of AFM layers compared to the original state after field cooling.[3] Normally, once the training effect occurred, it is not possible to recover the initial (untrained) hysteresis loop without raising the temperature above the Néel temperature followed by a repeated field cooling. Recently, Brems *et al.*[9] reported a surprising recovery of the training effect in Co/CoO bilayers without raising the temperature. Instead, by performing a hysteresis loop with the magnetic field perpendicular to the cooling field direction and measuring the hysteresis loops in the horizontal direction again, they found the training effect can be partially recovered. Utilizing anisotropic magnetoresistance (AMR) measurements, they found the degree of the recovery strongly depends on the magnitude of the applied perpendicular field.[9] With too low or too high perpendicular field, no training recovery was observed. The recovery occurs only within a certain field range. With increasing applied perpendicular field, the degree of the training recovery initially increases sharply, shows a peak, and further gradually decreases to zero. The authors explained the observed effect within the framework of the model of Fulcomer and Charp,[10] which was modified by Hou *et al.*[11] By assuming that the grains of the AFM layer have three easy axes and taking the collective behavior of 100 grains of randomly distributed easy axis, the model qualitatively yielded the experimental results.[12] But the responses of the individual grains with different easy axis orientations were not discussed. This, however, is important for understanding the effects in single-crystalline exchange bias systems which are fundamentally more interesting. Besides, paramagnetic CoO has a NaCl-type crystal structure. In the antiferromagnetic state it shows a tetragonal distortion along the cube edges.[13–15] Therefore, a fourfold instead of threefold symmetry is expected. And the fourfold anisotropy has been clearly visualized recently by photoelcetron emission microscopy (PEEM) combined with x-ray magnetic circular and linear dichroism (XMCD, XMLD).[16,17] Utilizing two independent magnetic sublattices for the antiferromagnet with multiple easy axes, Hoffmann numerically simulated the training effect within the coherent rotation model.[18] This model with biaxial (fourfold) AFM anisotropy was applied to explain the training effect of Co/CoO system successfully.

In this paper, we adopt Hoffmann's model and investigate the recovery of the training effect. For a single domain, we find training effect can be recovered only within a certain perpendicular field range. The field range strongly depends on the angle between the AFM easy axes and the applied field direction. Assuming a homogeneous distribution of the AFM easy axes, the asymmetry of the AMR as a function of the perpendicular field is calculated. The calculated AMR asymmetry initially shows a sharp increase with the perpendicular field and then gradually reduces to zero, in good agreement with the experimental findings.

## II. COMPUTATIONAL MODEL

We utilize the two sublattices AFM model in the calculations. The model has been successfully used to explain the

 

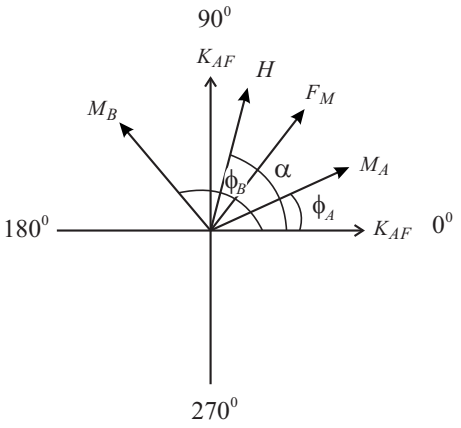


FIG. 1. Schematic of the relative orientation of the ferromagnet, the antiferromagnets, and their easy axes involved in the exchange bias system used for the calculations. The AFM has two equivalent magnetic easy axes (horizontal and vertical axes).

training effect by Hoffmann.[18] As experimentally, Co/CoO is the first investigated system which shows the training recovery effect, we follow the general character of this system in the simulations. CoO has a fourfold anisotropy due to its tetragonal structure.[13–15] Recent experiments shows that CoO typically has AFM domain structures and they overlap with the FM domains.[16,17] Therefore, in the simulations, we adopt the following assumptions: (1) the AFM has a fourfold anisotropy and it can be divided into two independent magnetic sublattices which both couple to the FM layer identically. (2) All magnetizations rotate coherently within the plane of the interface, which is the typical behavior of thin film without strong perpendicular anisotropy. (3) For simplicity, we initially neglect the anisotropy of the FM layer. The effect of the FM anisotropy will be discussed in the latter part. With these assumptions, the total energy of the system can be described as

$$E = -\mathbf{H}\cdot\mathbf{M}_F - J_I\mathbf{M}_F\cdot\sum_{i=A,B}\mathbf{M}_i - \mathbf{H}\cdot\sum_{i=A,B}\mathbf{M}_i - J_{AF}\mathbf{M}_A\cdot\mathbf{M}_B + K_{AF}M_{AF}[\sin^2(2\phi_A)+\sin^2(2\phi_B)],$$

where $\mathbf{H}$ is the external magnetic field, $\mathbf{M}_F$ is the magnetic moment of the FM layer, and $\mathbf{M}_A$ and $\mathbf{M}_B$ are the two AFM sublattice magnetic moments. $J_I$ is the exchange coupling between the FM layer and the two AFM sublattices, $J_{AF}<0$ is the AFM coupling between the two AFM sublattices. $K_{AF}$ is the anisotropy constant of the AFM layer, $M_{AF}=|\mathbf{M}_A|=|\mathbf{M}_B|$, and $\phi_A$ and $\phi_B$ are angles between each AFM sublattice magnetization and one of the easy axis directions, the external field has an angle $\alpha$ with respect to one of the easy axes of the AFM layer (see Fig. 1). The magnetic hysteresis loop can be obtained by calculating the minimum of the total energy. It is assumed that the system relax to the lowest global energy state after field cooling process. This global energy minimum is then the starting point of the first hysteresis loop. In the beginning, the parameters are tentatively set to be $|\mathbf{M}_F|=|\mathbf{M}_A|+|\mathbf{M}_B|$, $J_{AF}=-2.2J_I$, and $K_{AF}=0.5J_I|\mathbf{M}_F|$. The influence of the different ratios between the parameters will be discussed latter.

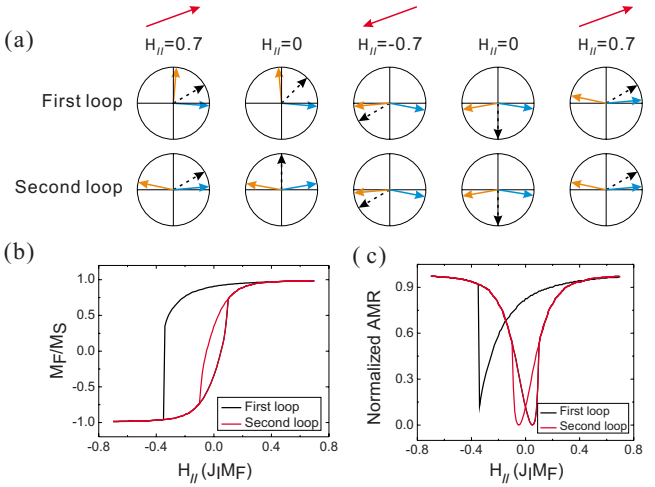


FIG. 2. (Color online) (a) The FM (dashed arrow) and each of the AFM sublattices magnetization (solid arrow) for saturation and at remanence during the first and second hysteresis loops after field cooling. The solid lines indicate the magnetic easy axes of the AFM. (b) Calculated first (black) and second (red) hysteresis loops after field cooling. The magnetization is normalized by the FM saturation magnetization $M_S$. (c) The corresponding AMR curves.

In the detailed experiments, Brems *et al.*,[9,12] studied the training recovery effect with four-point high-resolution AMR measurements. For a homogeneous ferromagnet, the AMR depends on the relative orientation between the electrical current and magnetization.[19] Mathematically, it can be written as

$$R(\beta) = R_\perp + R_0\cos^2(\beta),$$

where $\beta$ is the angle between the electrical current and the magnetization direction, $R_\perp$ is the resistance with all the magnetization perpendicular to the current, and $R_0$ is the difference in resistance with the magnetization parallel and perpendicular to the current, respectively. For a multidomain structure, one can calculate the resistance of each domain and estimate the total resistance according to their serial and/or parallel configurations. In our simulations, we use a serial configuration due to the sample geometry discussed below.

We first briefly describe the mechanism of the training effect using simulated results for $\alpha=\pi/9$ as an example. Figure 2(a) shows the field evolution of the magnetization orientations of the FM and the two AFM sublattices during the first and the second hysteresis loops after field cooling. Above $T_N$, the two AFM sublattices are randomly distributed and the magnetization of the FM should orientate along the field direction. While cooling in large field through $T_N$, the system should relax toward the global energy minimum state (ground state configuration). Due to the AFM coupling between the two AFM lattices, they prefer to be antiparallel to each other. Conversely, the exchange coupling between the FM with the two AFM sublattices favors a parallel configuration of the two AFM sublattices. The balance of these two couplings leads to a perpendicular configuration of the AFM sublattices, as shown in the left most panel of the first loop in

Fig. 2(a). When the field is reduced to zero, the FM orients its magnetization in the middle of the two perpendicular AFM sublattices (45° position) due to the exchange coupling with them. With increasing field in the reverse direction, the FM rotates further and switches to the almost opposite direction. During the FM rotation process, whether the AFM sublattices jump between two easy axes or not depends on the strength of the applied field. When the field is weak, none of the AFM sublattices switch to the other easy axis. If a strong field is applied, both AFM sublattices can rotate during the field sweeping. Only in an intermediate field range, $[H_1, H_2]$, one of the two AFM sublattices (the one that has the angle with the field direction in the range $[90°, 135°]$) can jump between two easy axes. With a magnetic field of $0.7J_I|\mathbf{M}_F|$, one of AFM sublattices rotates and the two AFM lattices become almost antiparallel to each other. During further sweeping of the field, the angles between the two AFM sublattices and the field direction remain either smaller than 90° or bigger than 135°, respectively. Therefore, after the first field reversal the AFM sublattices relax into a metastable antiparallel configuration and this configuration remains nearly unchanged for subsequent hysteresis loops, as shown in Fig. 2(a).

Figure 2(b) shows the calculated first and second hysteresis loops after field cooling. As discussed above, the switching details of the first and second loops are different. Therefore, different hysteresis loops (i.e., training effect) are obtained. The first hysteresis loop (black line) has a clear asymmetry, the magnetization reversal is abrupt while the second loop (red line) is more rounded and has no shift. The subsequent hysteresis loops are found to be essentially unchanged from the second hysteresis loop. From this simulation, one can find that the AFM sublattice magnetizations configuration plays a key role in the exchange bias and training effect.[18] Only when the AFM sublattice magnetizations are initially perpendicular to each other, the system exhibits the training effect. Figure 2(c) presents the correspondingly normalized AMR curves of the first and second hysteresis loops. During the first loop, the FM magnetization has an irreversible jump in the first-half loop and undergoes a reversible rotation process in the second half loop. In such case, the magnetization can be fully perpendicular to the applied field direction only in the second half loop [black line in Fig. 2(c)]. Therefore, the AMR only reaches zero in the second half loop and has nonzero value dip for the first half loop. On the contrary, the FM magnetization undergoes a reversible rotation process for both branches of the second loop and thus are perpendicular to the field direction at the coercive fields. As a result, both branches of the AMR curves reach zero during the second hysteresis loop.

## III. RESULTS AND DISCUSSION

In Sec. II, we discussed the basic mechanism of the training effect and its corresponding field-dependent AMR. In order to simulate the experimentally observed training recovery effect, we continue to present the influence of subsequent applied perpendicular field. For this, we perform similar hysteresis calculations as described above, but with a magnetic field ($H_\perp$) perpendicular to the cooling field following a trained loop along the cooling field direction. One can easily image that the training effect will not be reinduced if $H_\perp$ is too small to change the configuration of the AFM sublattice magnetizations. Therefore, we focus our discussions on an intermediate and a large perpendicular field case. As examples, the calculated results for $H_\perp = 0.7$ and 1.5 are presented in Fig. 3. As discussed in the previous paragraph, the two AFM sublattices orientate close to 0° and 180° after two consecutive hysteresis loops with fields along the cooling field direction. From the simulations described in previous paragraph, we deduce the following qualitative behavior: when the applied field is within an intermediate range, the AFM sublattices can rotate and jump to another easy axis only when the orientation between the sublattice magnetization and the applied field are in the range $[90°, 135°]$. So the two AFM sublattices are in the perpendicular configuration when $H_\perp = 0.7$. As the field is reduced again to zero, the FM orients its magnetization in the middle of the two perpendicular AFM sublattices (i.e., a 135° position) due to the exchange coupling with them. With increasing field in the reverse direction, one AFM sublattice (along 180°) will rotate to the other easy axis (along 270°), ending in an antiparallel configuration which remains nearly unchanged for subsequent hysteresis loop with the perpendicular field. As a result, after a hysteresis loop with $H_\perp = 0.7$, the AFM sublattices orientate nearly antiparallel to each other. One aligns along 90° and the other along 270°. With further increasing the magnetic field again in the cooling field direction (we call this a normal loop), the two AFM sublattices are perpendicular to each other again. In this case, the system goes back to the untrained state and the training effect can be recovered.

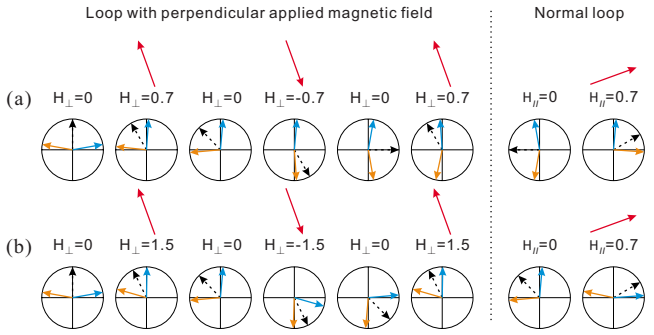


FIG. 3. (Color online) The FM (dashed arrow) and each of the AFM sublattices magnetization (solid arrow) for saturation and at remanence during the hysteresis loop when the magnetic field is applied perpendicular to the cooling field and half of the loop when the field is again along the direction of the cooling field. (a) $H_\perp = 0.7$. (b) $H_\perp = 1.5$.

As discussed above, if a strong perpendicular field larger than $H_2$ is applied (e.g., $H_\perp = 1.5$), the strong field will force the two AFM sublattices to be in a perpendicular configuration at the end of each loop. The two AFM sublattices remain perpendicular to each other after hysteresis loop with a perpendicular field, one aligns along 90° and the other one along 180°, see Fig. 3(b). With increasing the field in the cooling field direction again, one AFM sublattice (along 90°)

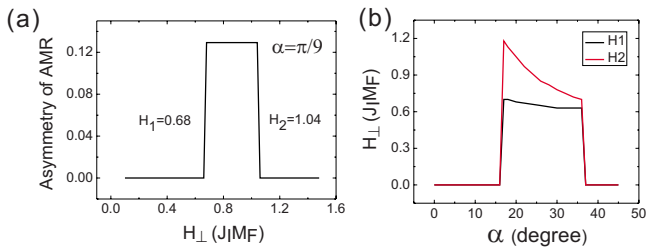


FIG. 4. (Color online) (a) $H_{\perp}$ dependence of the degree of the asymmetry of the AMR. The orientation between the cooling field and the easy axis of the AFM layer is $\alpha=\pi/9$. (b) Orientation between cooling field and easy axis of the AFM layer dependence of $H_1$ (black) and $H_2$ (red).

will jump to the other easy axis (0°). As a result, the two sublattices favor an antiparallel configuration and the training effect is not expected for a subsequent loop.

As shown in Fig. 3, the training effect can be recovered only when $H_{\perp}$ is within a certain range. To obtain the degree of training recovery, we further perform AMR calculations based on the simulated hysteresis loops. The asymmetry degree of the AMR is defined as the difference in depth of the AMR minima at both coercive fields divided by the change of AMR at the second coercive field.[12] To compare with the experimental results, we follow the same definition. The training induced asymmetry of the AMR as a function of the perpendicular field for $\alpha=\pi/9$ is presented in Fig. 4(a). We find the asymmetry of the AMR has a constant nonzero value within a specific field range. The lower and upper limit of the perpendicular field are defined as $H_1$ and $H_2$. For $\alpha=\pi/9$, $H_1=0.68$, and $H_2=1.04$. This is in contrast with the experimental results for the polycrystalline sample where a peak was obtained.[9]

For a polycrystalline sample, it is natural to image that it contains multiple grains with their easy in-plane axes oriented differently. Therefore, we further performed similar simulations for different $\alpha$. According to the symmetry, we will first discuss the situation for $\alpha$ from 0° to 45°. Figure 4(b) shows the calculated results. Interestingly we find $H_1$ and $H_2$ depend on $\alpha$. When $\alpha$ is below ≈17° and above ≈37°, both $H_1$ and $H_2$ are zero, namely there is no training recovery effect no matter how strong the perpendicular field is applied. Only when $\alpha$ is in the range of ≈17° to ≈37°, $H_1$ and $H_2$ are different. In such case, a training recovery is expected when the applied perpendicular field is larger than $H_1$ but smaller than $H_2$. In the discussed range, both $H_1$ and $H_2$ decrease with increasing $\alpha$ but with different slopes. $H_2$ initially has a larger value and decreases faster in comparison with $H_1$. In addition, the calculated asymmetry of AMR curve is not the same for different $\alpha$ within a certain $H_{\perp}$. Furthermore, the fact that the training effect recovery occurs only for certain values is consistent with the experimental observation that the untrained state is only partially recovered.[9]

In the previous paragraphs, we discussed the perpendicular field-induced training effect recovery of a single domain for different $\alpha$. Next we will consider the influence of domains for the experimental observation. The sample consist of stripes with 2 $\mu$m width and 120 $\mu$m length.[9] Thus the

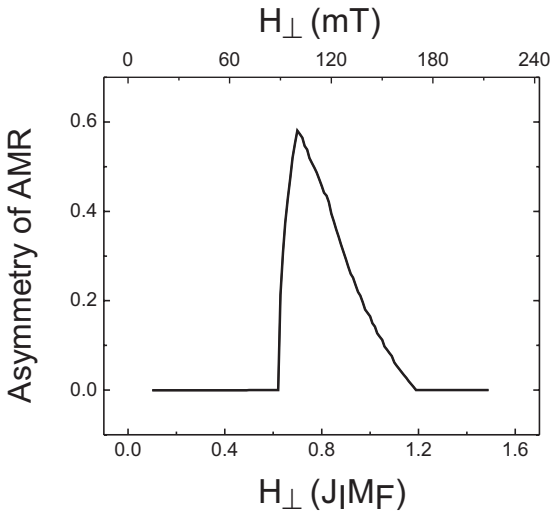


FIG. 5. Calculated degree of the asymmetry of the AMR along the cooling field after performing a hysteresis loop perpendicular to the cooling field direction. The horizontal axis corresponds to the maximum value of the perpendicular applied magnetic field ($H_{\perp}$). The corresponding fields for the simulated Co/CoO sample are marked on the top scale.

FM layer and AFM layers are very likely not in single domain state. Very recently, Miguel *et al.*, studied both the FM and AFM domain structures of wedge-shaped Fe layers on continuous CoO thin films by combining PEEM with XMCD and XMLD.[16] They found that the domains of the Fe layer are typically as large as tens of microns, coexisting with smaller domains of a few microns in size. Furthermore, an almost perfect overlap between FM and AFM domains was found. These results were further confirmed by a recent study.[17] One could expect a very similar situation in Co/CoO system. So in our calculations, we divided the sample into multidomains and assume each FM domain couples one AFM domain. In addition, the orientations of the easy axes of the different AFM domains are considered to be randomly distributed within the plane of the film. Based on the symmetry, first we consider $\alpha$ in the range $[0°,45°]$. We further assume that the domains are of the same size, 2 $\mu$m $\times$2 $\mu$m. In a 2-$\mu$m-wide stripe, it can be considered that all the FM domains are in a series configuration for the charge current. Therefore, the total AMR of the sample can be obtained by simply summing up the AMR of the different FM domains. The calculated degree of asymmetry of AMR of the whole sample is shown in Fig. 5. We find the training effect cannot be recovered at all when $H_{\perp}$ is below 0.62. The degree of the asymmetry quickly increases with further increasing the perpendicular field and the asymmetry reaches a maximum at $H_{\perp}\approx 0.7$. Then it decreases with a smaller slope and vanishes when $H_{\perp}$ is larger than 1.2. Interestingly, we find the simulated results follow the same field dependence as the experimental findings. To check the validity of the model, we also varied the ratio between $J_{AF}$ and $J_I$ and performed similar calculations. The essential features remain unchanged while the peak position depends almost linearly with their relative ratios. In addition, the peak position also depends on the ratio of $K_{AF}$ versus $J_I|\mathbf{M}_F|$. We find that the

larger the ratio is, the higher field where the peak appears.

In order to make a direct comparison with the experimental value for Co/CoO system, we also include the material parameters, $1.4\times10^6$ A/m for the Co magnetization and $5\times10^5$ J/m$^3$ for the CoO anisotropy constant.[20] In combination with the thickness of FM layer (20 nm), and the AFM layer (2 nm),[9] we can translate the normalized field into SI units. The calculated ratio is: $J_I|\mathbf{M}_F|\approx143$ mT for $J_{AF}=-2.2J_I$ and $K_{AF}=0.5J_I|\mathbf{M}_F|$. The corresponding fields for the simulated Co/CoO sample are marked on the top scale of Fig. 5. Interestingly, we find that not only the shape of calculated perpendicular field dependent AMR symmetry is similar to the experimental curve but also the peak position ($\approx100$ mT) and the intensity of the peak ($\approx0.6$) are almost the same as the experimental values (see Fig. 2 in Ref. 12). Due to the limit availability of specific parameters of Co/CoO system, the quantitative comparison, especially the peak position, is difficult. The similarity of the simulated results and the experimental findings suggests the validity of the model and one may use it to estimate the sample parameters which are experimentally hard to measure.

We note that the model used by Brems *et al.*,[12] also gives similar results. In their calculations, they assumed that the grains of the AFM layer have three easy axes and allowed the FM to couple with many AFM domains. This suggests that the training recovery effect occurs in the system that has multiple AFM easy axes. There is no strict limitation on system symmetry. Besides, our calculation shows a strong difference between the single domain case and the multidomain case. This points out the strong correlation between multidomain state with the observed effect. In addition, this difference may offer a check for the model if a single domain sample can be properly prepared.

In the following, we will continue to discuss the situation for $\alpha\in[45°,90°]$. When the $H_\perp$ is in the intermediate range, the magnetizations behave very similarly as the situation for $\alpha\in[0°,45°]$. For instance, when we set $\alpha=7\pi/18$ and $H_\perp=0.7$. If $H_\perp$ is not very large (e.g., $H_\perp=0.7$), the switching behavior is almost the same as the case for $\alpha=\pi/9$ and the training effect can be recovered (not shown). The situation can be different when a large perpendicular field (e.g., $H_\perp=1.5$) is applied. In this case, although the two AFM sublattices are still nearly perpendicular to each other at the end of the perpendicular hysteresis loop, the in-plane field is not strong enough to rotate any AFM sublattice to the other easy axis [see Fig. 6(a)]. The system is still in a metastable state instead of the ground state, and the AFM sublattices remain at 90°,180° in contrast to 0°,90° for $\alpha=\pi/9$. When a normal hysteresis loop is performed, the AFM sublattices change to the antiparallel configuration, the system exhibits training effect again [see Fig. 6(b) and 6(c)]. However, one can notice that the normalized magnetization $M_F/M_S$ of the first loop approaches zero reversibly. As a result, both of the two AMR curves reach zero as its minimum, resulting in a zero asymmetry of AMR [see Fig. 6(d)]. The minimum of the first AMR curves is often achieved under different field for different $\alpha$. If we sum up all contributions of different $\alpha$ between [0°,90°], a negative asymmetry will be obtained when $H_\perp>1.0$ (as shown in Fig. 7 as black curve), which is not observed in the experiments.

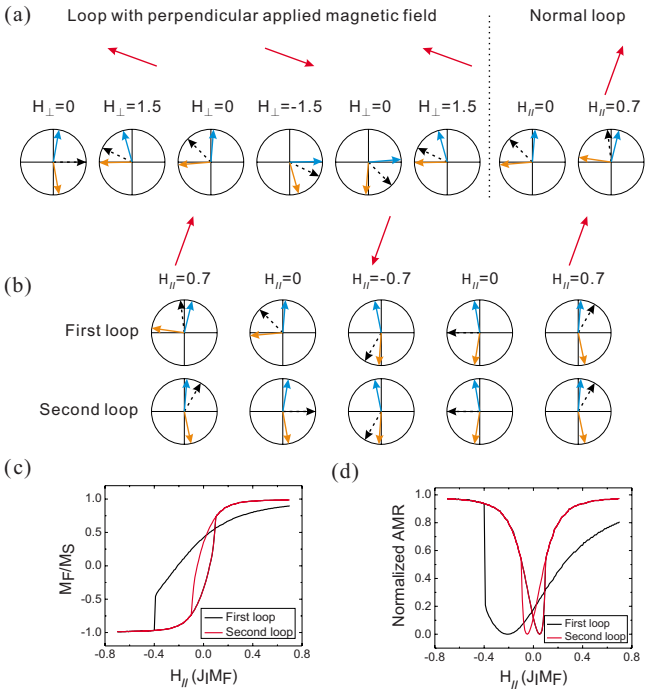


FIG. 6. (Color online) (a) The FM (dashed arrow) and each of the AFM sublattices magnetization (solid arrow) for saturation and at remanence during the hysteresis loop when the magnetic field is applied perpendicular to the cooling field and half of the loop when the field is again along the direction of the cooling field. (b) The FM and the two AFM sublattices magnetization for saturation and at remanence during the first and second hysteresis loops after the procedure in (a). (c) Calculated first (black) and second (red) hysteresis loops. (d) The corresponding AMR curves.

The difference between our simulated results and experiments may come from the assumptions, which we adopted for simplifying the simulations. In our calculations, the anisotropy of the FM layer is ignored and only in-plane coher-

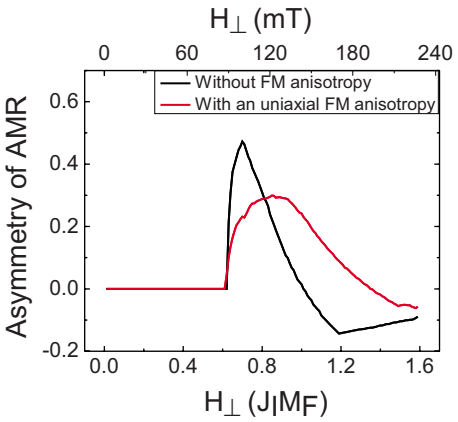


FIG. 7. (Color online) Calculated degree of the asymmetry of the AMR along the cooling field after performing a hysteresis loop perpendicular to the cooling field direction. The horizontal axis corresponds to the maximum value of the perpendicular applied magnetic field ($H_\perp$). The black curve represents results when there is no anisotropy in the FM layer and red curve represents results when an uniaxial anisotropy of the FM layer is included.

ent rotation is considered. In reality, the FM layer may naturally have a certain magnetic anisotropy. In Hoffmann's calculations, a better quantitative agreement between the experimental data and the simulated hysteresis loops can be achieved by adding an FM anisotropy.[18] We performed similar calculations by adding an uniaxial anisotropy ($K_F = 0.15K_{AF}$) to the FM layer, with its easy direction 45° away from the cooling field. The calculated result is shown in Fig. 7 (red curve). We find that the negative asymmetry is significantly decreased though the peak also decreases a little bit after this modification. Besides, the switching process may occur through three-dimensional rotation[21] or the domain nucleation and domain-wall propagation. When these mechanisms are included, better agreement between theoretical simulations and experimental observations may be obtained.

## IV. SUMMARY

We performed numerical simulations of the perpendicular magnetic field-induced training recovery effect with multiple AFM easy axes. Both the FM and AFM layers are divided into multiple domains, and each FM domain couples with only one AFM domain. We find that the training effect can be recovered after performing a hysteresis loop with perpendicular field. The possibility to reinduce the training effect strongly depends on the applied field strength. The calculated perpendicular field dependent AMR asymmetry increases with the field sharply and gradually reduces to zero, in good agreement with the experimental findings. The nice agreements between the calculations and the experimental results indicate that the perpendicular field induced training recovery effect likely occurs in systems with the training effect between the first and the second loop. Furthermore, as we did not use any specific parameters of Co/CoO in our model, we expect that the same physics should occur in any system that shows training effect due to multiple easy axes in the antiferromagnet, e.g., commonly used metallic antiferromagnets, such as FeMn. Our calculations suggest that the training recovery effect is mainly related to the field-dependent AFM sublattice orientation, which can change between different easy axes. We also note that although our model mainly described the case for a spin compensated surface of the antiferromagnet. When a small imbalance between the magnetizations of the two AFM sublattices (uncompensated case) is considered, we find the main results remain essentially the same.

## ACKNOWLEDGMENTS

The authors acknowledge the fruitful discussion with A. Hoffmann and W. Y. Zhang. This work is supported by NSFC (Grants No. 10604026, No. 10834001, No. 10874076, and No. 10974087), NCET, and the State Key Programme for Basic Research of China (Grants No. 2007CB925104 and No. 2010CB923401).

*Corresponding author; hfding@nju.edu.cn

[1] W. H. Meiklejohn and C. P. Bean, Phys. Rev. **102**, 1413 (1956).
[2] J. Nogués, J. Sort, V. Langlais, V. Skumryev, S. Suriñach, J. S. Muñoz, and M. D. Baró, Phys. Rep. **422**, 65 (2005).
[3] J. Nogués and I. K. Schuller, J. Magn. Magn. Mater. **192**, 203 (1999).
[4] A. E. Berkowitz and K. Takano, J. Magn. Magn. Mater. **200**, 552 (1999).
[5] M. Kiwi, J. Magn. Magn. Mater. **234**, 584 (2001).
[6] D. Paccard, C. Schlenker, O. Massenet, R. Montmory, and A. Yelon, Phys. Status Solidi **16**, 301 (1966).
[7] C. Binek, Phys. Rev. B **70**, 014421 (2004).
[8] S. Polisetty, S. Sahoo, and C. Binek, Phys. Rev. B **76**, 184423 (2007).
[9] S. Brems, D. Buntinx, K. Temst, C. Van Haesendonck, F. Radu, and H. Zabel, Phys. Rev. Lett. **95**, 157202 (2005).
[10] E. Fulcomer and S. H. Charap, J. Appl. Phys. **43**, 4190 (1972).
[11] C. Hou, H. Fujiwara, K. Zhang, A. Tanaka, and Y. Shimizu, Phys. Rev. B **63**, 024411 (2000).
[12] S. Brems, K. Temst, and C. Van Haesendonck, Phys. Rev. Lett. **99**, 067201 (2007).
[13] N. C. Tombs and H. P. Rooksby, Nature (London) **165**, 442 (1950).
[14] S. Greenwald, Acta Crystallogr. **6**, 396 (1953).
[15] W. Jauch, M. Reehuis, H. J. Bleif, F. Kubanek, and P. Pattison, Phys. Rev. B **64**, 052102 (2001).
[16] J. Miguel, R. Abrudan, M. Bernien, M. Piantek, C. Tieg, J. Kirschner, and W. Kuch, J. Phys.: Condens. Matter **21**, 185004 (2009).
[17] J. Wu, J. S. Park, W. Kim, E. Arenholz, M. Liberati, A. Scholl, Y. Z. Wu, C. Y. Hwang, and Z. Q. Qiu, Phys. Rev. Lett. **104**, 217204 (2010).
[18] A. Hoffmann, Phys. Rev. Lett. **93**, 097203 (2004).
[19] I. A. Campbell and A. Fert, in *Ferromagnetic Materials*, edited by E. P. Wohlfarth (North-Holland, Amsterdam, 1982), Vol. 3.
[20] S. Chikazumi, *Physics of Ferromagnetism* (Oxford University Press, New York, 1997).
[21] P. Biagioni, A. Montano, and M. Finazzi, Phys. Rev. B **80**, 134401 (2009).